# Microstructural and magnetic properties of thin obliquely deposited films: A simulation approach

P.N. Solovev [a,b,*], A.V. Izotov [a,b], B.A. Belyaev [a,b,c]

[a] Kirensky Institute of Physics, Siberian Branch of the Russian Academy of Sciences, 50/38, Akademgorodok, Krasnoyarsk 660036, Russia
[b] Siberian Federal University, 79, pr. Svobodnyi, Krasnoyarsk 660041, Russia
[c] Reshetnev Siberian State Aerospace University, 31, pr. Imeni Gazety "Krasnoyarskii Rabochii", Krasnoyarsk 660014, Russia

ABSTRACT

The relation between microstructural and magnetic properties of thin obliquely deposited films has been studied by means of numerical techniques. Using our developed simulation code based on ballistic deposition model and Fourier space approach, we have investigated dependences of magnetometric tensor components and magnetic anisotropy parameters on the deposition angle of the films. A modified Netzelmann approach has been employed to study structural and magnetic parameters of an isolated column in the samples with tilted columnar microstructure. Reliability and validity of used numerical methods is confirmed by a good agreement of the calculation results with each other, as well as with our experimental data obtained by the ferromagnetic resonance measurements of obliquely deposited thin $Ni_{80}Fe_{20}$ films. The combination of these numerical methods can be used to design a magnetic film with a desirable value of uniaxial magnetic anisotropy and to extract the obliquely deposited film structure from only magnetic measurements.

## 1. Introduction

Thin magnetic films with heterogeneous microstructure have gained much attention over the last decades. This interest is driven by the aim of a fundamental understanding of the thin films magnetism and their great potential applications in the fields of magnetic sensors, high-density data storage, and microwave devices. From practical point of view, it is of great importance to have a possibility to specifically engineer their magnetization configuration and magnetization dynamics. One way of adjusting magnetic properties of thin films is to modify artificially their microstructure [1–3]. Among all approaches offering a possibility to influence thin films microstructure, oblique deposition is one of the simplest methods of producing films with controllable morphology [4,5]. In oblique deposition, an atom flux strikes the substrate surface at a non-normal incidence. Consequently, the formed on the substrate at the initial stage of the film growth nuclei (Volmer-Weber growth mode is assumed) cast "shadows" in the direction parallel to the atoms flux. The competition between geometrical shadowing and surface diffusion leads to the growth of the tilted columnar microstructure, which character strongly depends on the deposition angle (an angle between an atoms flux and a film normal) [6,7].

The oblique deposition results in films with intrinsically anisotropic physical properties [8]. Particularly, it was established many years ago

[9,10] that the oblique metal deposition induced a uniaxial magnetic anisotropy in resulting thin polycrystalline magnetic films. Experiments showed that the uniaxial magnetic anisotropy strength could be controlled by the deposition angle. It was also demonstrated that, depending on the deposition angle, in-plane easy axis could be oriented either perpendicular or parallel to the incidence plane of the atoms flux, and the reorientation occurred for incidence angles typically above 60–70°. The oblique deposition technique is now used widely to produce multilayers [11] and exchange bias systems [12] with different magnetic anisotropy in individual layers, to control magneto-transport properties of granular films [13], or to tune magneto-optical properties of slanted columnar thin films [14]. It is also a promising method for fabrication of thin films and multilayers with high ferromagnetic resonance frequencies suitable for modern microwave applications [15–17].

Thus, it is important to understand better the relation between microstructure and magnetic behavior of these obliquely deposited thin films. In the case of ultrathin films, the oblique deposition mainly affects only surface roughness leading to the formation of surface ripples in the samples [18,19]. In these works it was shown, that using atomic-force (AFM) or scanning tunneling microscopy data of the films surface profile as input, the magnetostatic energy associated with these surface corrugations and consequently the strength of the magnetic

anisotropy induced by oblique deposition could be calculated. However, in thicker obliquely deposited films magnetic anisotropy is crucially governed by the columnar microstructure [7,20], and it is challenging to characterize experimentally this buried structures throughout films volume [20,21]. Therefore, to explore theoretically a behavior of a magnetic anisotropy related to columnar microstructure simple phenomenological models [22] or models of films consisting of regularly arranged and tilted ellipsoidal particles [23] were considered. More recently, an interesting approach was used to study numerically optical [24] and electrical [25] properties of obliquely deposited thin films with complex columnar morphology. In this approach, three-dimensional structures predicted by a thin film growth simulator were analyzed using different numerical technics to study their electrical conductivity and optical transmission. The reasonably good agreement between numerical and experimental results demonstrated the perspectives of this method that offers opportunities not only to reproduce but also to predict some properties of thin films with nonuniform morphology.

The aim of this work is to investigate numerically the relation between inclined columnar microstructure and static magnetic properties of thin obliquely deposited magnetic films. A feature of our work is the utilization of a Monte Carlo thin film growth simulator to produce the three-dimensional thin-film structures for simulations of their magnetic properties. The relation between the deposition angle and a uniaxial magnetic anisotropy induced by dipole-dipole interactions in the oblique films is firstly examined, with the comparison between numerical results and experimental data. Then, the original [26] and a modified Netzelmann approaches are used for analysis of the simulated oblique films properties.

## 2. Methods

### 2.1. Experiment

In order to calibrate parameters of the film growth model and also to compare simulated results with experimental data, we fabricated obliquely deposited thin permalloy films with different incidence angles, similar to the experiments performed by Smith et al. [9] and Cohen [10]. Thin-film samples were produced by thermal vacuum evaporation of $Ni_{80}Fe_{20}$ on polished glass $10\times10\times0.5$ mm size substrates at room temperature. The base pressure was lower than $10^{-6}$ mbar and the deposition rate was 1 nm/s. The substrates were tilted so that the deposition beam struck the surface at an angle $\alpha$ with respect to the film normal. The deposition angle $\alpha$ was in the range 0–75°. During the deposition, an external in-plane magnetic field $H=200$ Oe oriented perpendicularly to the deposition plane was applied. The nominal thickness of each sample was 40 nm. Note that in oblique deposition, an effective area of the sample decreases and its porosity enhances as deposition angle increases [4]. Therefore, to keep the thicknesses of the resulting films approximately equal we adjusted a time of deposition. Magnetic properties of the produced samples were measured by the scanning spectrometer of ferromagnetic resonance (FMR), where the microstrip resonator fabricated on a dielectric substrate was used as a sensor [27]. The measurements were performed at the fixed microwave pump frequencies 2.27 GHz and 3.33 GHz on the local areas (spot with diameter ~1 mm) of the samples. The uniaxial in-plane magnetic anisotropy of the films was retrieved from the obtained angular dependences of the resonance field by fitting the theoretical model of a film to the experimental data [28].

### 2.2. Film growth simulation

To study numerically the correlation between magnetic and microstructural properties of obliquely deposited thin films, we developed a thin film growth simulator [29] allowing us to generate three-dimen-

sional (3D) structures with columnar morphology reproducing that of experimental obliquely deposited films. Our simulation code is based on simple ballistic deposition models previously reported elsewhere [30,31], which employ a Monte Carlo approach to model the diffusion-limited aggregation process. The simulation region is represented as a rectangular lattice of cubic cells, each with a volume of $\Delta^3$. A thin film is considered as the aggregate of cubic particles (growth units), each occupying a cubic cell. At a first stage of the simulation, a flat substrate represented by cubic particles occupying the lower layer is generated. Then, particles are launched sequentially toward the substrate from randomly chosen in-plane $(x,y)$ coordinates and with the initial height ($z$ coordinate) just above the film surface. The particles descend on a linear trajectory that is determined by the deposition angle $\alpha$ (the angle between the deposition direction and the substrate normal). Each particle moves until it finds itself near the substrate or the surface of the film. In real deposition process, immediately before reaching the film surface the deposited atoms deviate from their initial linear trajectories because of interatomic interactions (for instance Van der Waals forces) with surface atoms [32,33]. To include these effects to some degree in our simple model, we applied two conditions at which a deposited particle ceases its movement and incorporates in the film. (i) If among particle's nearest neighbor cells at least a one cell is non-empty (occupied), the particle incorporates in the film with the probability 1. (ii) If among particle's next nearest neighbor cells at least a one cell is non-empty, the particle might join to this occupied cubic cell with the probability 0.5.

After a particle is deposited, it is then allowed to diffuse over the film surface. The diffusion algorithm is based on a simple random walk model [30]. The diffusing particle hops from site to site (nearest vacancies) with a total number of the hops $S$. The probability of the particle to diffuse from its current position $i$ to the nearest vacancy $j$ depends on the vacancy's number $N_j$ of the nearest neighbors (non-empty cells) and is defined as follows [30].

$$P_{i\to j} = \frac{\exp(\gamma N_j)}{\sum_{j_{total}} \exp(\gamma N_j)}, \qquad (1)$$

where $\gamma$ is a constant, and the summation is taken over all allowed vacancies ($j_{total}$). From the physical point of view, $\gamma$ is a coefficient that represents the ratio between the surface energy and the film temperature while $S$ defines the diffusion length that is related mainly to the deposition rate and the film temperature. Usually, due to complex nature of real evaporation process, the initial parameters of the simulation are calibrated against experimentally measured characteristics of real films [31]. In this work, we adjusted model parameters such that calculated magnetic anisotropy of simulated structures fitted best to the measured anisotropy of obliquely deposited thin permalloy films. Consequently, we found that $\gamma=0.45$ and $S=5$. Similar to Ref. [25], by comparing the average column diameter of the simulated structures with that of experimental obliquely deposited Py films, we estimated the size of a single cubic particle as $\Delta=0.5$ nm. Note that in the simulator we implemented periodic boundary conditions in the surface plane for the deposition and diffusion processes. We modeled the oblique deposition of thin-film structures of size $256(x)\times256(y)\times80(z)$ $\Delta$ for a set of deposition angles in the range 0°–85°. In order to improve the reliability of the obtained results, for each deposition angle $\alpha$ ten independent simulations of a film growth were performed. Hence, values in the figures that will be presented in Section 3 are the average characteristics of these ten films (for each $\alpha$) while the error bars indicate the range of values (when no error bar is shown, the error was less than the symbol size).

### 2.3. Evaluation of the simulated films magnetic properties

To evaluate the magnetic properties of the simulated thin-film structures, we employed a Fourier space approach proposed by

Beleggia and De Graef [34], which allows for calculation of the demagnetizing tensor field for a magnetic object with an arbitrary shape. In this approach, the complex problem of the magnetic vector potential calculation is simplified by transition from real space to the Fourier space, where the calculation of the vector potential transforms from a convolution operation to a vector product. The shape of the magnetic object can be described by its shape function $D(\mathbf{r})$ (where $\mathbf{r}$ is a radius vector in real space) [34], which equals to unity in the regions of space occupied by the magnetic object and equals to zero outside the object. Since produced by the film growth simulator structures are represented as three-dimensional arrays of zeroes (voids) and ones (particles), these 3D arrays are the discrete representations of the shape functions [35]. It was shown, that the volume averaged demagnetizing tensor (or magnetometric tensor) of an object with the shape function $D(\mathbf{r})$ could be calculated using the following expression

$$N_{ij} = \frac{1}{8\pi^3 V} \int d^3\mathbf{k} \frac{|D(\mathbf{k})|^2}{k^2} k_i k_j, \tag{2}$$

where $V$ is the volume of a magnetic object, $D(\mathbf{k})$ is the Fourier transform of the shape function (shape amplitude), and $\mathbf{k}$ is the frequency vector. Note that the magnetometric tensor can be also considered as a demagnetizing tensor of an equivalent ellipsoid for the investigated films [36]. We performed fast Fourier transform of the 3D arrays, which represented simulated obliquely deposited films and then, by using Eq. (2) we calculated numerically $N_{ij}$ for each sample.

## 3. Results

### 3.1. Magnetic anisotropy

Thin-film structures produced by the simulation exhibit a columnar microstructure, as it can be seen from Fig. 1a, where pseudo-AFM images of films surface (see Ref. [25]) and pseudo-TEM (transmission electron microscopy) images of films cross-sections (see Ref. [24]) deposited at angles α=45° and α=80° are shown. The simulated structures are similar to that observed in real obliquely deposited thin magnetic films, as it can be seen from presented in Fig. 1b high-resolution TEM cross-section image of Py film deposited at α=45°. In our previous work [29], we have investigated in detail the morphology of these simulated oblique films. It have been shown that the samples density monotonically decreased and the tilt of the columns increased with increasing deposition angle. Furthermore, as revealed by statistical analyses of the films structure, both the columns distribution over the films surface and the shape of the columns cross-section became increasingly anisotropic as deposition angle increased.

In order to understand how this columnar morphology influences magnetic properties of the films, we have analyzed magnetometric tensors numerically calculated for each simulated film. Generally, the principal axes of the magnetometric tensors do not coincide with the axes of the original coordinate system $xyz$, where $z$ axis is normal to the film plane and $y$ axis is parallel to the incidence (deposition) plane. Diagonalization of the calculated $N_{ij}$ tensors revealed that the orthogonal transformation from the $xyz$ system to a new coordinate system $x'y'z'$ which axes coincide with the principal axes of the magnetometric tensor can be realized by the rotation about the $x$ axis by an angle θ, as it is shown in Fig. 1c. Fig. 1c also sketches the cross-section of the equivalent ellipsoid in $x'y'$ plane. The calculations show that the component (demagnetization factor) $N_z$ of the diagonalized magnetometric tensor is about ten times larger (on average) than the $N_x$ and $N_y$ components, although the difference between them slowly decreases as deposition angle increases (Fig. 2).

Therefore, in a moderate external magnetic field the magnetization of the film will lie in the $x'y'$ plane, which can be referred to as an "easy" plane. In this case, the field $H_k$ of the magnetic uniaxial anisotropy originating from dipole-dipole interactions can be evaluated from:

$$H_k = M_s(N_y - N_x), \tag{3}$$

where $M_s$ is the magnetization saturation of the film. For our calculations, we use the magnetization saturation value typical for permalloy ($Ni_{80}Fe_{20}$): $M_s$=860 G. Note that if $H_k$ is positive, the easy axis of the magnetization is parallel to the $x'$ axis, otherwise it is parallel to the $y'$ axis.

Fig. 3 shows the calculated uniaxial anisotropy field $H_k$ as a function of the deposition angle α (square symbols). For comparison, the uniaxial magnetic anisotropy measured by the FMR spectrometer for the obliquely deposited thin permalloy films are also plotted (circles). The observed character of $H_k(\alpha)$ dependence is related to the two processes occurring during film growth: columns aggregation and film's density decay. The oblique deposition of particles, because of the shadowing effect and limited surface diffusion, leads to the growth of columns which tend to coalescence in the direction perpendicular to the deposition plane, thus leading to the formation of the magnetization easy axis parallel to this direction ($N_y > N_x$). However, as the oblique deposition angle increases, the porosity of the resulting films enhances and for α > 75° the shape of individual columns become to play a crucial role. Here, to minimize the magnetostatic energy, the magnetization has to orient towards the long axis of the columns ($N_y < N_x$). The easy axis thus lies parallel to the deposition plane and is inclined at an angle θ with respect to the film surface (see inset in Fig. 3), with the inclination angle that depends on both a film packing density and a tilt of columns.

### 3.2. Modified Netzelmann approach

In this section, we propose a modification of the Netzelmann theory [26], and apply this modified approach to analyze microstructural properties of the simulated films. The demagnetizing energy of heterogeneous magnetic objects, such as investigated here obliquely deposited films with columnar microstructure, can be evaluated in the framework of the Netzelmann theory. Netzelmann assumed [26] that the demagnetizing energy of a particulate magnetic film could be expressed as a combination of energies of the two limiting cases: an isolated particle with a demagnetization tensor $N^e$ and a homogeneously magnetized film with a demagnetization tensor $N^t$. If we denote by $\mathbf{M}$ the magnetization vector and by $p$ the packing factor, which defines the relative fraction of magnetic particles in the sample, and take into account corrections made by Dubowik [37,38] and Kakazei [39,40], the magnetostatic energy density can be written as

$$F_d = \frac{1}{2}p(1-p)\mathbf{M}N^e\mathbf{M} + \frac{1}{2}p^2\mathbf{M}N^t\mathbf{M}. \tag{4}$$

The first term on the right-hand side of Eq. (4) is the magnetic energy associated with the shape of the particles, and the second term is the demagnetizing energy related to the overall geometry of the sample. In this case, the demagnetizing field is given by

$$\mathbf{H}_d = -\frac{1}{p}\frac{dF_d}{d\mathbf{M}} = -(1-p)N^e\mathbf{M} - pN^t\mathbf{M} = -N\mathbf{M}, \tag{5}$$

where the magnetometric demagnetizing tensor of the sample is

$$N = (1-p)N^e + pN^t = N^e + p(N^t - N^e). \tag{6}$$

This last expression is of great practical importance, since one can use it to determine demagnetizing factors of an individual particle of the assembly of equal, homogeneously distributed particles constituting the film. In the coordinate system which $z$ axis coincides with the film normal the demagnetizing tensor $N^t$ has only one non-zero component $N_{zz}^t = 4\pi$. If the packing factor $p$ and the magnetometric tensor of the sample are known, we can easily find the demagnetizing tensor of a single particle as

$$N^e = (N - pN^t)/(1-p). \tag{7}$$
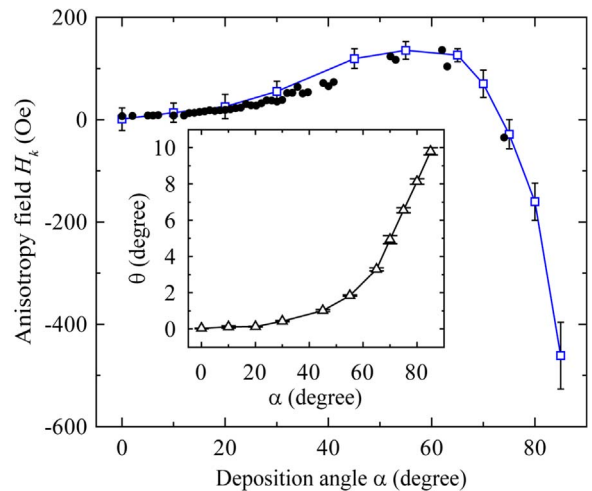
Thus, we can use the Netzelmann approach to determine the
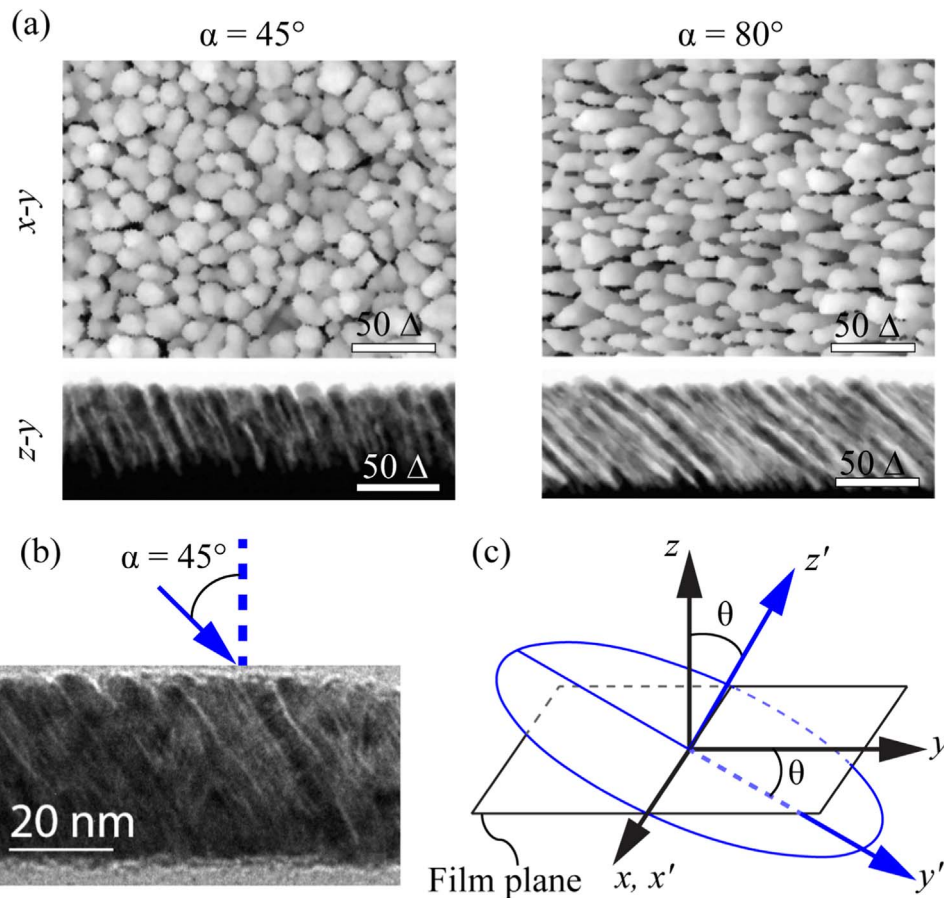
**Fig. 1.** (**a**) Surface (*x-y*) and cross-section (*z-y*) images of the films simulated for incidence angles α=45° and α=80°. (**b**) TEM cross-section image of Py film deposited at α=45°. (**c**) Coordinate systems: *xyz* represents the film coordinate system, and *x′y′z′* represents the coordinate system of the diagonalized magnetometric tensor of the film.
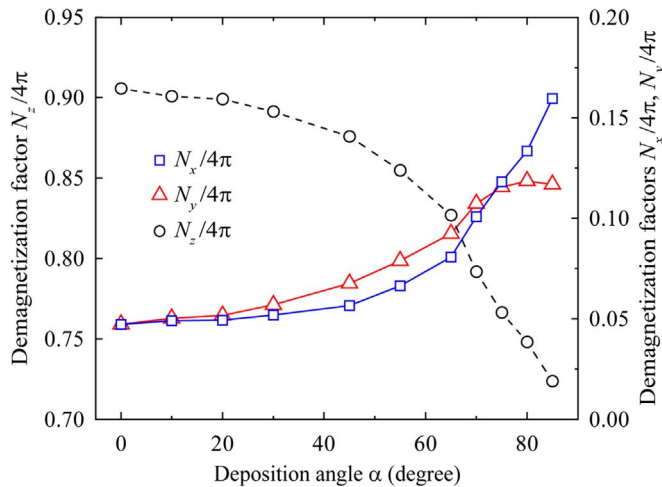


**Fig. 2.** Components (demagnetization factors) of the diagonalized magnetometric tensor calculated for simulated films as a function of the deposition angle α.



**Fig. 3.** Dependence of the uniaxial anisotropy field $H_k$ on the deposition angle α. Square symbols show results of the calculations for simulated films, while solid circles are the experimental data measured for obliquely deposited Py films. Inset shows easy axis inclination angle θ (with respect to the film surface) obtained for simulated films as a function of the deposition angle α.

average parameters of an isolated (individual) column in obliquely deposited films. However, it is important to notice that the Netzelamnn theory assumes that the particles distributed homogeneously inside the film [40]. While this is the case for particulate magnetic films, the experimental measurements and simulation results demonstrate that the obliquely deposited films have a variation in density over their thickness, with density usually decreasing from the film substrate to top [41–43]. In other words, the packing factor or packing density of the obliquely deposited films is the function of the layer coordinate

$p=p(z)$. As an example, inset in Fig. 4 shows the distribution of the simulated films packing density over their thickness.

We therefore should modify the original Netzelmann theory to take into account the dependency of the films packing density on their thickness. For this, let us divide the sample into $n$ layers with equal thicknesses. In this case, the demagnetizing field energy will be
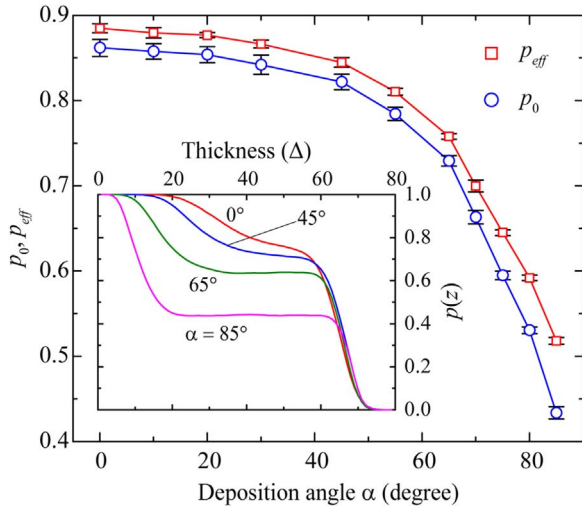
**Fig. 4.** The average packing density $p_0$ and effective packing density $p_{eff}$ of the simulated films as a function of the deposition angle α. Inset shows packing density $p$ as a function of the film thickness plotted for several deposition angles.



**Fig. 5.** Components of a diagonalized demagnetizing tensor $N^e/4\pi$ of an isolated column as a function of the deposition angle. Solid lines show results obtained with the modified Netzelmann approach ($p= p_{eff}$), and dashed lines show results obtained with the original Netzelmann approach ($p= p_0$).

$$F_d = \frac{1}{2n} \sum_{i=1}^{n} p_i(1 - p_i)\mathbf{M}N^e\mathbf{M} + \frac{1}{2n} \sum_{i=1}^{n} p_i^2 \mathbf{M}N^t\mathbf{M}, \tag{8}$$

where $p_i$ is the packing density of layer $i$, while the overall sample's packing density is $p_0 = \frac{1}{n}\sum_{i=1}^{n} p_i$. By introducing an effective packing factor $p_{eff} = \sum_{i=1}^{n} p_i^2 / \sum_{i=1}^{n} p_i$, we obtain the following expression for the demagnetizing field

$$\mathbf{H}_d = -\frac{1}{p_0}\frac{dF_d}{d\mathbf{M}} = -(1 - p_{eff})N^e\mathbf{M} - p_{eff}N^t\mathbf{M}. \tag{9}$$

Notice that Eq. (9) can be obtained from Eq. (5) through a simple replacement of $p$ by $p_{eff}$. Therefore, we can write an analogous to Eq. (7) expression for the determination of the demagnetizing tensor of an individual column in the obliquely deposited thin film

$$N^e = (N - p_{eff}N^t)/(1 - p_{eff}). \tag{10}$$

The average packing density $p_0$ and effective packing density $p_{eff}$ of the simulated films are plotted as a function of the deposition angle α in Fig. 4. It can be seen that $p_{eff}$ is just a bit larger (about 5%) than $p_0$. However, this leads to the noticeable correction when calculating demagnetizing tensors. This is demonstrated by Fig. 5, where the components of a diagonalized demagnetizing tensor of an individual column are shown as a function of the deposition angle. Here, the components calculated with Eq. (7) (i.e. for $p= p_0$) are depicted by dashed lines, while the components calculated with Eq. (10) (i.e. for $p=p_{eff}$) are depicted by solid lines.

Transformation of the demagnetization tensor $N^e$ to its principal axes allow us to determine the average tilt of the long axis of a separate column in the sample about $z$ axis. Fig. 6a presents angles of columns tilt β (measured with respect to the film normal) plotted against the deposition angle α, which were calculated using the original ($p=p_0$) and the modified ($p=p_{eff}$) Netzelmann approach. Fig. 6a also shows results obtained from autocorrelation structural analysis of the simulated films [29]. One can see that in the case $p=p_{eff}$ the calculated from magnetic parameters angles of the columns tilt almost identical to the values obtained directly from the structural analysis, while in the case $p=p_0$ the obtained angles have a large dispersion and exceed the structural data on about 10°.

If we assume that the columns in the simulated oblique films may be approximated by elongated cylinders with an elliptic cross-section, it is then possible to calculate from the demagnetizing tensors $N^e$ a cross-section aspect ratio of the column. Using analytical expressions for the tensor components $N_x^e$ and $N_y^e$ of an elongated elliptic cylinder [44], we
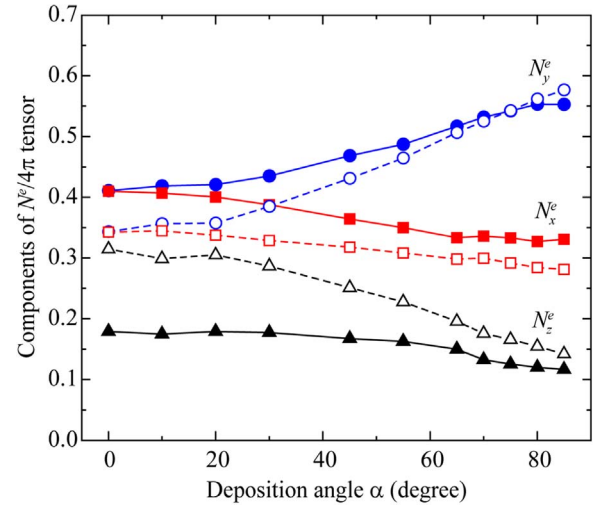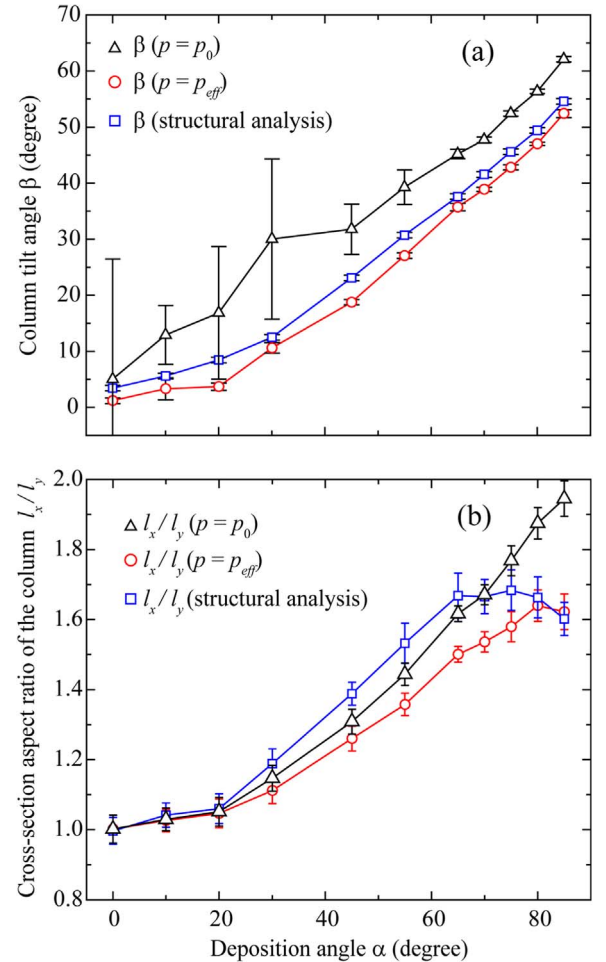


**Fig. 6.** (a) Column tilt angle β and (b) cross-section aspect ratio of the column $l_x/l_y$ as a function of the deposition angle. In both figures, we present results derived from the demagnetizing tensor $N^e$ using the original ($p= p_0$) and the modified ($p= p_{eff}$) Netzelmann approach, and we also show data retrieved from structural statistical analysis of the simulated films.

calculate its cross-section aspect ratio $l_x/l_y$ for the samples simulated with different deposition angles (Fig. 6b). As in the previous case, we used the $N^e$ tensors obtained with the original and the modified Netzelmann approach. Fig. 6b also shows aspect ratio $l_x/l_y$ derived from the two-dimensional autocorellation functions calculated for the simulated structures [29]. It can be seen, that the $l_x/l_y$ ratio calculated from demagnetizing tensors for both cases differs from values obtained by structural statistical analysis. However, the character of $l_x/l_y(\alpha)$ dependences obtained for $p = p_{eff}$ accords with the data obtained from structural statistical analysis better than that calculated for $p = p_0$. We note that the observed in Fig. 6b difference between aspect ratio values obtained from structural analysis and values calculated from demagnetizing tensors could be due to anisotropic distribution of columns over the films surface.

## 4. Conclusion

In this work, by combining thin film growth simulations and the Fourier space approach for calculation of the magnetometric tensors, we investigated in detail the relationship between microstructural and magnetic properties of the obliquely deposited films. We showed that by appropriate choice of the initial parameters of the quite simple growth model it was possible to generate columnar thin-film structures with magnetic uniaxial anisotropy induced by dipolar mechanism that accurately reproduced anisotropy of real samples. With the magnetometric demagnetizing tensors of the simulated films in hand, we also demonstrated that the Netzelamnn theory may be used to retrieve information about microstructure of obliquely deposited films (average columns tilt and columns cross-section aspect ratio) by analyzing their magnetic characteristics. The proposed modification of the Netzelamnn approach, which took into account films packing density variations over their thickness, allowed us to obtain structural data that are more accurate comparing to the data obtained with the original approach. These findings can be used in practice to study the averaged structural parameters of obliquely deposited magnetic films by analyzing their integral magnetic characteristics measured, for example, by means of ferromagnetic resonance.

## Acknowledgements

## References

[1] J.Fassbender, T.Strache, M.O.Liedke, D.Marko, S.Wintz, K.Lenz, A.Keller, S. Facsko, I.Mönch, J.McCord, Introducing artificial length scales to tailor magnetic properties, New Journal of Physics, vol. 11, 2009, p. 125002. ⟨http://dx.doi.org/10.1088/1367-2630/11/12/125002⟩.

[2] R. Gallardo, A. Banholzer, K. Wagner, M. Körner, K. Lenz, M. Farle, J. Lindner, J. Fassbender, P. Landeros, Splitting of spin-wave modes in thin films with arrays of periodic perturbations: theory and experiment, New J. Phys. 16 (2014) 023015. http://dx.doi.org/10.1088/1367-2630/16/2/023015.

[3] T. Maity, S. Li, L. Keeney, S. Roy, Ordered magnetic dipoles: controlling anisotropy in nanomodulated continuous ferromagnetic films, Phys. Rev. B 86 (2012) 024438. http://dx.doi.org/10.1103/PhysRevB.86.024438.

[4] M.M. Hawkeye, M.T. Taschuk, M.J. Brett, Glancing Angle Deposition of Thin Films: Engineering the Nanoscale, John Wiley & Sons, 2014. http://dx.doi.org/10.1002/9781118847510.

[5] A. Barranco, A. Borras, A.R. Gonzalez-Elipe, A. Palmero, Perspectives on oblique angle deposition of thin films: from fundamentals to devices, Progr. Mater. Sci. 76 (2016) 59–153. http://dx.doi.org/10.1016/j.pmatsci.2015.06.003.

[6] L. Abelmann, C. Lodder, Oblique evaporation and surface diffusion, Thin Solid Films 305 (1997) 1–21. http://dx.doi.org/10.1016/S0040-6090(97)00095-3.

[7] H. Kranenburg, C. Lodder, Tailoring growth and local composition by oblique-incidence deposition: a review and new experimental data, Mater. Sci. Eng. R11 (1994) 295–354. http://dx.doi.org/10.1016/0927-796X(94)90021-3.

[8] M.M. Hawkeye, M.J. Brett, Glancing angle deposition: Fabrication, properties, and applications of micro- and nanostructured thin films, J. Vac. Sci. Technol. A 25 (2007) 1317. http://dx.doi.org/10.1116/1.2764082.

[9] D.O. Smith, M.S. Cohen, G.P. Weiss, Oblique incidence anisotropy in evaporated Permalloy films, J. Appl. Phys. 31 (1960) 1755. http://dx.doi.org/10.1063/1.1735441.

[10] M.S. Cohen, Anisotropy in permalloy films evaporated at grazing incidence, J. Appl. Phys. 32 (1961) S87. http://dx.doi.org/10.1063/1.2000509.

[11] M. Maicas, R. Ranchal, C. Aroca, P. Sanchez, E. Lopez, Magnetic properties of permalloy multilayers with alternating perpendicular anisotropies, Eur. Phys. J. B 62 (2008) 267–270. http://dx.doi.org/10.1140/epjb/e2008-00163-4.

[12] A.B. Oliveira, R.L. Rodriguez-Suarez, S. Michea, H. Vega, A. Azevedo, et al., Angular dependence of hysteresis shift in oblique deposited ferromagnetic/ antiferromagnetic coupled bilayers, J. Appl. Phys. 116 (2014) 033910. http://dx.doi.org/10.1063/1.4890457.

[13] G.N. Kakazei, A.F. Kravetz, N.A. Lesnik, M.M. Pereira de Azevedo, Yu.G. Pogorelov, G.V. Bondarkova, V.I. Silantiev, J.B. Sousa, Influence of co-evaporation technique on the structural and magnetic properties of CoCu granular films, J. Magn. Magn. Mater. 196–197 (1999) 29–30. http://dx.doi.org/10.1016/S0304-8853(98)00648-9.

[14] D. Schmidt, T. Hofmann, C. Herzinger, E. Schubert, M. Schubert, Magneto-optical properties of cobalt slanted columnar thin films, Appl. Phys. Lett. 96 (2010) 091906. http://dx.doi.org/10.1063/1.3340913.

[15] X. Zhu, Z. Wang, Y. Zhang, L. Xi, J. Wangn, Q. Liu, Tunable resonance frequency of FeNi films by oblique sputtering, J. Magn. Magn. Mater. 324 (2012) 2899–2901. http://dx.doi.org/10.1016/j.jmmm.2012.04.035.

[16] J. Vergara, C. Favieres, V. Madurga, Increased ultra high frequency magnetic susceptibility in nanopatterned nanolayers with strong exchange coupling, J. Phys. D: Appl. Phys. 48 (2015) 435003. http://dx.doi.org/10.1088/0022-3727/48/43/435003.

[17] A. Bonneau-Brault, S. Dubourg, A. Thiaville, S. Rioual, D. Valente, Adjustable ferromagnetic resonance frequency in CoO/CoFeB system, J. Appl. Phys. 117 (2015) 033902. http://dx.doi.org/10.1063/1.4904510.

[18] J. Wolfe, R. Ling, W. Kawakamia, Z. Qiu, R. Arias, D. Mills, Roughness induced in plane uniaxial anisotropy in ultrathin Fe films, J. Magn. Magn. Mater. 232 (2001) 36–45. http://dx.doi.org/10.1016/S0304-8853(01)00016-6.

[19] J.L. Bubendorff, S. Zabrock, G.G.S. Hajjar, R. Jaafar, et al., Origin of the magnetic anisotropy in ferromagnetic layers deposited at oblique incidence, Europhys. Lett. 75 (1) (2006) 119–125. http://dx.doi.org/10.1209/epl/i2006-10089-5.

[20] C. Quiros, L. Peverini, J. Diaz, A. Alija, C. Blanco, M. Velez, et al., Asymmetric grazing incidence small angle x-ray scattering and anisotropic domain wall motion in obliquely grown nanocrystalline Co films, Nanotechnology 25 (2014) 335704. http://dx.doi.org/10.1088/0957-4484/25/33/335704.

[21] K. Krause, D. Vick, M. Malac, M. Brett, Taking a little off the top: nanorod array morphology and growth studied by focused ion beam tomography, Langmuir 26 (22) (2010) 17558–17567. http://dx.doi.org/10.1021/la103070x.

[22] J.M. Alameda, M. Torres, F. Lopez, On the physical origin of in-plane anisotropy axis switch in oblique-deposited thin films, J. Magn. Magn. Mater. 62 (1986) 209–214. http://dx.doi.org/10.1016/0304-8853(86)90146-0.

[23] E. Munster, Calculation of the magnetic properties of oblique-incidence thin films, J. Magn. Magn. Mater. 92 (1990) 279–283. http://dx.doi.org/10.1016/0304-8853(90)90644-6.

[24] K. Kaminska, M. Suzuki, K. Kimura, Y. Taga, K. Robbie, Simulating structure and optical response of vacuum evaporated porous rugate filters, J. Appl. Phys. 95 (2004) 3055. http://dx.doi.org/10.1063/1.1649804.

[25] D. Vick, M.J. Brett, Conduction anisotropy in porous thin films with chevron microstructures, J. Vac. Sci. Technol. 24 (2006) 156–165. http://dx.doi.org/10.1116/1.2148413.

[26] U. Netzelmann, Ferromagnetic resonance of particulate magnetic recording tapes, J. Appl. Phys. 68 (1990) 1800. http://dx.doi.org/10.1063/1.346613.

[27] B.A. Belyaev, A.V. Izotov, A.A. Leksikov, Magnetic imaging in thin magnetic films by local spectrometer of ferromagnetic resonance, IEEE Sens. 5 (2) (2005) 260–267. http://dx.doi.org/10.1109/JSEN.2004.842293.

[28] B.A. Belyaev, A.V. Izotov, P.N. Solovev, Competing magnetic anisotropies in obliquely deposited thin permalloy film, Physica B 481 (2016) 86–90. http://dx.doi.org/10.1016/j.physb.2015.10.036.

[29] B.A. Belyaev, A.V. Izotov, P.N. Solovev, Growth simulation and structure analysis of obliquely deposited thin films, Russ. Phys. J. 59 (2016) 301. http://dx.doi.org/10.1007/s11182-016-0771-2.

[30] M. Suzuki, Y. Taga, Numerical study of the effective surface area of obliquely deposited thin films, J. Appl. Phys. 90 (2001) 5599. http://dx.doi.org/10.1063/1.1415534.

[31] T. Smy, D. Vick, M.J. Brett, S.K. Dew, A.T. Wu, J.C. Sit, K.D. Harris, Three-dimensional simulation of film microstructure produced by glancing angle deposition, J. Vac. Sci. Technol. 18 (2000) 2507–2512. http://dx.doi.org/10.1116/1.1286394.

[32] S. Muller-Pfeiffer, H. Kranenburg, J.C. Lodder, A two-dimensional Monte Carlo model for thin film growth by oblique evaporation: simulation of two-component systems for the example of Co-Cr, Thin Solid Films 213 (1992) 143–153. http://dx.doi.org/10.1016/0040-6090(92)90489-X.

[33] R. Alvarez, L. Gonzalez-Garcia, V.R.P. Romero-Gomez, et al., Theoretical and experimental characterization of $TiO_2$ thin films deposited at oblique angles, J. Phys. D: Appl. Phys. 44 (2011) 385302. http://dx.doi.org/10.1088/0022-3727/44/38/385302.

[34] M. Beleggiaa, M.D. Graef, On the computation of the demagnetization tensor field for an arbitrary particle shape using a Fourier space approach, J. Magn. Magn. Mater. 263 (2003) L1–L9. http://dx.doi.org/10.1016/S0304-8853(03)00238-5.

[35] S. Tandona, M. Beleggiab, Y. Zhub, M.D. Graef, On the computation of the demagnetization tensor for uniformly magnetized particles of arbitrary shape. Part II: numerical approach, J. Magn. Magn. Mater. 271 (2004) 27–38. http://dx.doi.org/10.1016/j.jmmm.2003.09.010.

[36] M. Beleggia, M.D. Graef, Y.T. Millev, The equivalent ellipsoid of a magnetized body,

J. Phys. D: Appl. Phys. 39 (2006) 891–899. http://dx.doi.org/10.1088/0022-3727/39/5/001.

[37] J. Dubowik, Shape anisotropy of magnetic heterostructures, Phys. Rev. B 54 (1996) 1088. http://dx.doi.org/10.1103/PhysRevB.62.727.

[38] J. Dubowik, Erratum: shape anisotropy of magnetic heterostructures [Phys. Rev. B 54, 1088 (1996)], Phys. Rev. B 62 (2000) 727. http://dx.doi.org/10.1103/PhysRevB.62.727.

[39] G.N. Kakazei, A.F. Kravets, N.A. Lesnik, M.M. Pereira de Azevedo, Yu.G. Pogorelov, J.B. Sousa, Ferromagnetic resonance in granular thin films, J. Appl. Phys. 85 (1999) 5654. http://dx.doi.org/10.1063/1.369830.

[40] D.S. Schmool, R. Rocha, J.B. Sousa, J.A.M. Santos, G.N. Kakazei, The role of dipolar interactions in magnetic nanoparticles: ferromagnetic resonance in discontinuous magnetic multilayers, J. Appl. Phys. 101 (2007) 103907. http://dx.doi.org/10.1063/1.2733630.

[41] B.C. Hubartt, X. Liu, J.G. Amar, Large-scale molecular dynamics simulations of glancing angle deposition, J. Appl. Phys. 114 (2013) 083517. http://dx.doi.org/10.1063/1.4819446.

[42] K. Kaminska, A. Amassian, L. Martinu, K. Robbie, Growth of vacuum evaporated ultraporous silicon studied with spectroscopic ellipsometry and scanning electron microscopy, J. Appl. Phys. 97 (2005) 013511. http://dx.doi.org/10.1063/1.1823029.

[43] A. Amassian, K. Kaminska, M. Suzuki, L. Martinu, K. Robbie, Onset of shadowing-dominated growth in glancing angle deposition, Appl. Phys. Lett. 91 (2007) 173114. http://dx.doi.org/10.1063/1.2794420.

[44] D. Goode, G. Rowlands, The demagnetizing energies of a uniformly magnetized cylinder with an elliptic cross-section, J. Magn. Magn. Mater. 267 (2003) 373–385. http://dx.doi.org/10.1016/S0304-8853(03)00406-2.